Building Simulation 2005

Ninth International IBPSA Conference
Montréal, Canada
August 15-18, 2005

MODELING THE PERFORMANCE OF PERSONALIZED VENTILATION UNDER DIFFERENT ROOM AIRFLOWS

Naiping Gao*, Jianlei Niu
Department of Building Services Engineering, The Hong Kong Polytechnic University, Hung Hom, Kowloon, Hong Kong, China
*Corresponding author. Tel: 852 2766 4698 E-mail: 02902469r@polyu.edu.hk

ABSTRACT

Personalized ventilation (PV) has the ability to improve inhaled air quality and accommodate the individual thermal preference. In this paper one kind of personalized ventilation system which supplies fresh air at the microphone position is investigated numerically. A numerical thermal manikin with the real geometry of human body is used to study the airflows around the occupant equipped with PV. The performance of one RNG k-ε model and the standard k-ε model is compared. The benefits of PV under different uniform room ambient flow are analyzed. The results indicate that the orientation of the human body to the uniform flow plays a key role.

INTRODUCTION

The aim of HVAC is to provide thermal comfort and good air quality at a low energy cost. At present total-volume ventilation and air-conditioning systems, such as mixing ventilation system and displacement ventilation system, are applied in most buildings. However individual thermal preferences can not be accommodated by these systems. Fresh supply air is polluted by building materials and bio-effluents before it is inhaled by the occupants. Personalized ventilation (PV) can improve the inhaled air quality, perceived air quality, and thermal comfort greatly (Zhu et al. 2003, Kaczmarczyk 2003) because it supplies fresh air directly to the breathing zone and only aims to control the individual micro-environment. By now the application of PV can be found primarily in USA, Japan and Europe, and researches on PV have been carried out in Lawrence Berkeley Laboratory, University of California at Berkeley, Denmark Technical University, etc. Since the performance of PV is greatly dependent on the different airflows around the human body detailed analysis of the micro-environment surrounding the body is essential. Heated thermal manikin (HTM) has been used to investigate the fraction of personalized air in the inhaled air (Melikov et al. 2002). With the development of computational fluid dynamics (CFD) the numerical thermal manikin (NTM) was developed in the study of local thermal comfort (Huang 2002). SØrensen and Voigt (2003) modeled the convective and radiative heat transfer from human body segments using a NTM with the accurate geometry of the real body.

In this paper we widen the application of the NTM to the study of PV. The results of using the standard k-ε model and a renormalization k-ε model (Yakhot and Orszag 1986) in modeling micro-environment around human body are compared. Then the impacts of room airflow on the performance of PV are analyzed.

CFD METHODS

All the detailed skin surface characteristics and human body extremities are obtained by using 3-D laser scanning technique to create the NTM. The NTM surface is composed by small patches with an average size of 4 mm. This NTM is placed at the center of a displacement ventilated room (Figure 1). The personalized ventilation air terminal device (ATD) is located at the microphone position beneath the chin. The ventilated room is divided into two parts for grids generation: a cuboid enclosing the human body and the remained room space. The cuboid is broken with unstructured grids (tetrahedral cell topology) while the other is discretized with structured grids. The total number of cells is 1,812,114. The real transient respiration process is simplified into a steady inhalation process with inhaled air rate of 0.14 l/s. Tracer gas CO_2 is mixed into the room supply air and personalized air, with respective concentration of 500 ppm and 4000 ppm, to characterize the inhaled air quality. Boundary conditions are listed in Table 1. Totally six cases are studied (Table 2).

In the previous numerical simulations of airflows around human body with a complex geometry a low Reynolds number k-ε model was used (Murakami et al. 1997; SØrensen and Voigt 2003; Voigt 2001). However Betts and Dafa'Alla (1986) made a comparison of different low Reynolds number k-ε models for predicting buoyant flow and found that no models could produce a completely satisfactory result. Voigt (2001) tried to use a constant eddy viscosity model after he failed to obtain convergence using the low Reynolds number k-ε model. But the differences between the simulation results and experiments were out of the acceptable range.

In the present study of airflows around the human body in case 1 the Rayleigh number Ra reaches about 4.1×10^9 at the head level, indicating the airflow at the upper part of the body can be regarded as turbulent flow. At the feet level the air speed is very low and the flow is laminar. Therefore the selection of the standard k-ε model or the RNG k-ε model (Yakhot and Orszag 1986) is a compromise. The aim is to determine the preferable turbulence model between them.

RESULTS AND DISCUSSION

Comparison of turbulence models

The air flow field, temperature field and tracer gas concentration distribution are selected in the comparison of these two turbulence models. The seated body in a calm environment is clearly observed to be covered with a warm upward airflow. The magnitude of the air velocity right above the head is shown in Figure 2. In the experiment and simulation by Murakami (2002) the peak value of the overhead upward airflow was approximately 0.20 m/s. In the present modeling this air speed is lower than 0.20 m/s. The reason should be that the body posture in the Murakami's study is standing. The values from SØrensen and Voigt (2003) are much higher. They used a low Reynolds number k-ε model to simulate the micro-environment around a seated human body in a uniform upward room airflow with the speed of 0.02 m/s. The much higher value may be due to the temperature of the ambient room air which is 2.25 ℃ lower than in present simulation. The above head air speed by the RNG k-ε model is a little higher than that by standard k-ε model although they are very close. This can be clearly observed by examining the room air flow filed. As illustrated in Figure 3 the core of the warm rising thermal plume with the maximum air speed is not right above the head due to the asymmetric seated body shape in the direction from back to front. The phenomenon was validated in the simulation by SØrensen and Voigt (2003). The smooth vertical surface of the back conduces to forming the warm upward flow which leads to the flow direction above head deflects to the back of the human body. The above head warm flow is thinner and stronger by the RNG k-ε model than that by the standard k-ε model although the maximum speed is same, namely 0.26 m/s. This is because for the RNG k-ε model in present simulation of natural convection the combined impact of the additional term R in the ε equation and other parameters including C_1, C_2, σ_k, σ_ε, C_μ which are different from those in the control equations of the standard k-ε model results in decreased turbulent viscosity. Gan (1998) evaluated the performances of the RNG k-ε model and the standard k-ε model in the prediction of turbulent buoyant flow. He pointed out that the RNG k-ε model performed better than the standard k-ε model because of the inclusion of the rate-of-stain term R. Other modifications of the turbulence constants, such as C_2, σ_k, σ_ε, also contributed to the improvement.

Figure 4 shows the air velocity boundary layer behind the human body at the neck region. The thickness of the velocity boundary layer is about 10 cm. In the simulation of a standing human body (Murakami et al. 1997) this thickness is 15 cm while in the experiment of air movement at the neck of a seated human body it is 8-9 cm (Melikov and Zhou 1996) which is a little smaller than the value in the present simulation. The maximum velocity in the boundary layer by the RNG k-ε model is larger than that by the standard k-ε model. This result can also be found in the numerical investigation by Gan (1998).

One index, namely personal exposure reduction (PER), expressed as the fraction of personalized air in the inhaled air, is employed to assess the pollutant concentration reduction in the inhalation from the average room air. The value of PER is 72.4% in case 1. Figure 5 illustrates the concentration levels of the tracer gas CO_2 in the region around the nose and the outlet of the weak jet flow. The tracer gas concentration in ambient room air and PV supply air is 500 and 4000 ppm respectively. It can be observed that large concentration gradients exist and the accurate prediction of this concentration distribution is essential for the evaluation of the PV performance. In contrast to the different performances of the standard k-ε model and the RNG k-ε model in the prediction of buoyant flow, the concentrations at the facial region are almost the same.

In the following study of PV under different uniform flow the standard k-ε model is used based on three reasons. Firstly the selection between these two models is of minor importance in relation to grids distribution. Secondly the CPU time for the RNG k-ε model is more than that for the standard k-ε model. In regard to present cases with 1,812,114 cells one thousand iterations require about 13.5 hours for the RNG k-ε model and 11 hours for standard k- ε model on a SUN ULTRA 60 workstation with five processors running at the speed of 400 MHz. Thirdly in the simulation of the interaction of the weak jet flow from PV and the thermal plume the results of the tracer gas concentration levels around the nose are almost same and our emphasis is the facial concentration level and the inhaled air quality with PV.

Effects of room air movement

Personalized ventilation should be integrated into a background air-conditioning system. The air movement caused by this secondary air-conditioning system affects the micro-environment around human

body and the performance of PV. Melikov et al. (2003) compared the ventilation effectiveness when PV was combined into mixing ventilation and displacement ventilation. In their experiments the PV always protected the occupant from pollution in rooms with mixing ventilation, but when applied with displacement ventilation the PV can either improve or decrease the inhaled air quality. Ambient air movement is of primary importance to temperature and pollutant concentration field around human body. Hyldgaard (1994) placed a thermal manikin as pollutant source in a horizontal uniform airflow to study the pollutant transportation and flow characteristics of the respiration air. He found that the horizontal uniform airflow at the speed of 0.05 m/s was able to bring away the exhaled air. Even airflow with velocity of 0.05-0.10 m/s can prevent the build up of the thermal plume on the windward side of the body. If the back was turned against the uniform flow the inhalation can still be taken from the rising convection flow as was the case in still ambient air. In the experiment by Melikov and Zhou (1996) it was found that an invading flow at the mean speed of 0.1 m/s and with turbulence intensity of 10% was able to penetrate the enclosing free convection flow.

In this series of numerical study the human body is placed in a uniform airflow, respectively approaching from the left, the front, the back, and the floor at the velocity of 0.2 m/s. Figure 6 shows the temperature fields. The warm rising flow at the windward side of the body is obviously torn away by the horizontal invading airflow irrespective of the flow direction. At the leeward of the human body the warm rising airflow still exists. The mean convective heat transfer coefficient of the body in the airflow from the front, the left, the back, and the floor at the speed of 0.2 m/s is 5.06, 5.31, 5.20, and 5.02 W/(m^2℃) respectively. These values are reasonable when compared with the simulation by Murakami et al. (1997) in which the mean convective heat transfer coefficient was 7.1 and 13 W/(m^2℃) when the human body with simplified geometry was placed in a uniform airflow at the speed of 0.25 m/s with the turbulence intensity of 6% and 29% individually.

The PER is compared in Figure 7. When the human body faces the uniform airflow the inhaled air is partially from PA and partially from the invading airflow due to the breaking of the thermal plume at the windward (Figure 8). The weak PV jet flow deflects to the face by the impinging of the ambient airflow. When the ambient air flows from the left to the right at the speed of 0.2 m/s the inhaled air is almost totally from the uniform airflow horizontally. The PV jet flow is blown away. In this situation the potential flow of the inhalation is completely enclosed by the invading airflow. When the uniform airflow is from the back, the inhalation is the mixture of the air from PV and the air from the thermal plume due to the protection of the warm rising flow at the leeward provided by the human body. The room air can flow through the gap between the legs which confines the form of the thermal plume to the body parts from the abdomen to the head. When room air supplies from the floor the uniform upward room airflow reduces the room temperature level if compared with case 1 and consequently intensifies the thermal plume around the body. In this situation the PER is lower than one in case 1.

CONCLUSION

The micro-environment around an occupant equipped with a personalized ventilation jet in a displacement ventilated room is simulated by using a numerical thermal manikin with the geometry of a real human body. Inhaled air quality, denoted by pollutant exposure reduction index, is used to evaluate the performance of PV.

RNG k-ε model and the standard k-ε model are compared, and it was found that, for buoyant flow, the warm upward airflow above the head simulated by the RNG k-ε model is slightly thinner and stronger than the one by the standard k-ε model. For the jet flow the tracer gas concentration distribution in the facial region resulted from the interaction of the thermal plume and PV airflow is almost the same by using these two models. The CPU time for the RNG k-ε model is slightly more than that for the standard k-ε model.

Room air movement at the speed of 0.2 m/s is strong enough to tear away the protection of the thermal plume at the windward of the body. The orientation of the human body to the wind is of primary importance to the value of PER. The uniform airflow from the left is able to blow away PA and leads to that the PER value is almost zero.

ACKNOWLEDGMENTS

The project is funded by the Research Grant Committee of the Hong Kong SAR government, under the project No. PolyU5031/01E. The authors also wish to thank Dr. Daniel Chan for the acquisition of the thermal manikin, and Miss Josephine Lau and Dr David T.W.Chan for their assistance in the laser-scanning of the thermal manikin.

REFERENCES

Betts, P.L., and Dafa'Alla, A.A. 1986. Turbulent buoyant airflow in a tall rectangular cavity. ASME Winter Annual Meeting, Anaheim, California, HTD-vol.60, pp.83-91.

Gan, G.H. 1998. Prediction of turbulent buoyant flow using an RNG k- ε model. Numerical Heat Transfer, Part A, Vol.33, no.2, pp.169-189.

Huang, L.J. 2002. Passenger thermal comfort model helps optimize HVAC systems, http://www.cfdreview.com/application/02/08/30/1422240.shtml.

Hyldgaard, C.E. 1994. Human as a source of heat and air pollution. Proceedings of ROOMVENT'94, the 4th International Conference on Air Distribution in Rooms, Krakow, Poland, Vol.1, pp.413-433.

Kaczmarczyk, J. 2003. Human response to personalized ventilation. PhD thesis, Department of Mechanical Engineering, Technical University of Denmark.

Melikov, A.K., and Zhou, G. 1996. Air movement at the neck of the human body. Proceedings of Indoor Air'96, the 7th International Conference on Indoor Air Quality and Climate, Nagoya, Japan, Vol.1, pp. 209-214.

Melikov, A.K., Cermak, R., Majer, M. 2002. Personalized ventilation: evaluation of different air terminal devices. Energy and Buildings, Vol.34, pp. 829-836.

Melikov, A.K., Cermak, R., Kovar, O., and Forejt, L. 2003. Impact of airflow interaction on inhaled air quality and transport of contaminants in rooms with personalized and total volume ventilation. Proceedings of Healthy Buildings 2003, Singapore, pp. 592-597.

Murakami, S. 2002. CFD study on the micro-environment around the human body with inhalation and exhalation, Proceedings of ROOMVENT2002, the 8th International Conference on Air Distribution in Rooms, Copenhagen, Denmark, pp. 23-35.

Murakami, S., Kato, S., and Zeng, J. 1997. Flow and temperature fields around human body with various room air distribution, CFD study on computational thermal manikin-part Ⅰ. ASHARE Transactions, Vol.103, part.1, pp.3-15.

SØrensen, D.N., and Voigt, L.K. 2003. Modeling flow and heat transfer around a seated human body by computational dynamics. Building and Environment, Vol.38, no.6, pp.753-762.

Voigt, L.K. 2001. Navier-Stokes simulations of airflow in rooms and around a human body. Ph.D. thesis, Technical University of Denmark.

Yakhot, V., and Orszag, S. 1986. A renormalization group analysis of turbulence. Journal of Scientific Computing, Vol.1, no.1, pp.1-51.

Zhu, S., Kato, S., Song, D., Murakami, S., and Sudo, M. 2003. Study on the personal air-conditioning system considering human thermal adaptation. Proceedings of 4th International Symposium on HVAC, Beijing, China, October 9-11, Vol.2, pp.393-401.

FIGURES AND TABLES

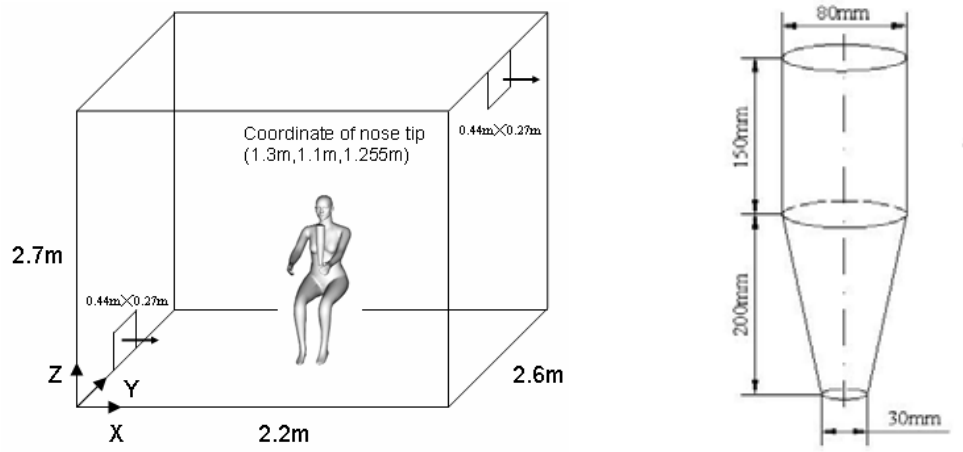

Figure 1 Thermal manikin in a displacement ventilated room and geometry of the ATD

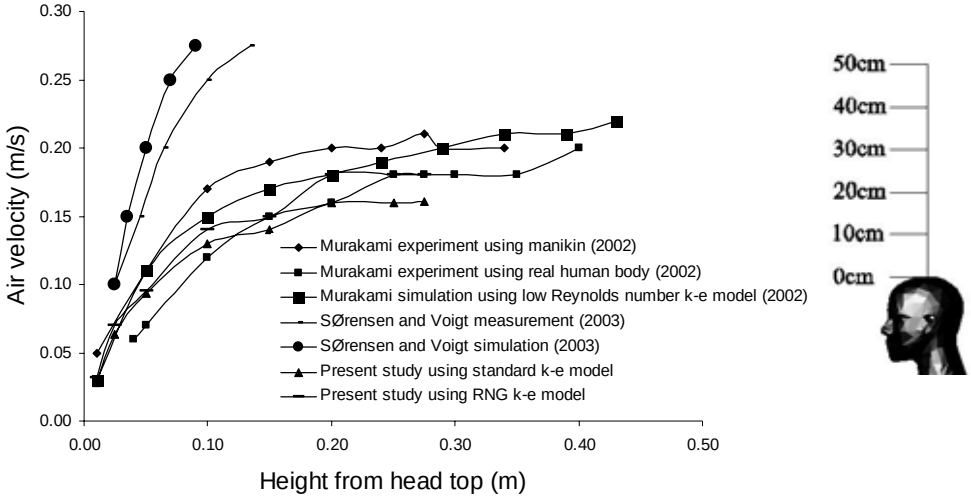

Figure 2 Comparison of air speed above the head in calm ambient air

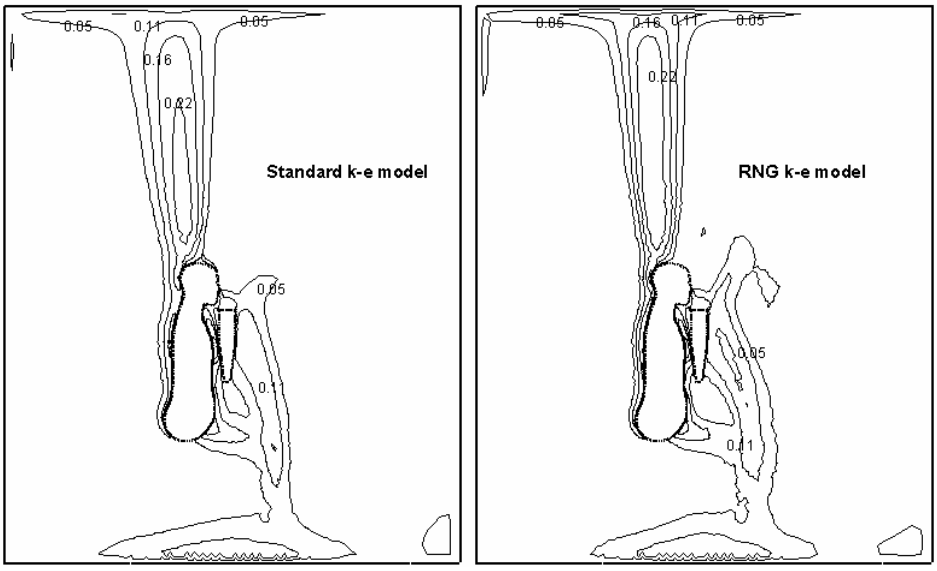

Figure 3 Air speed (m/s) contour at the middle surface (x=1.3 m)

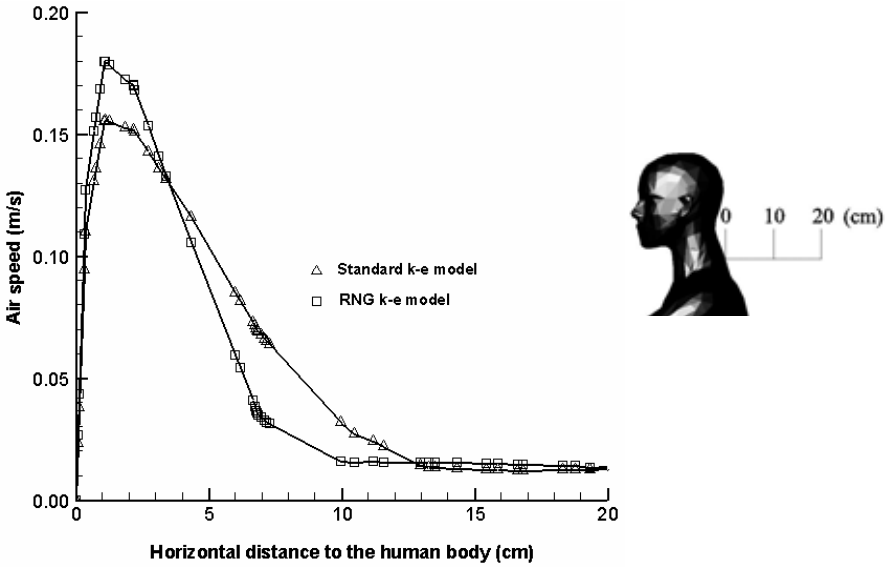

Figure 4 The magnitude of the air velocity at the neck right behind the human body (the height of about 1.10 m)

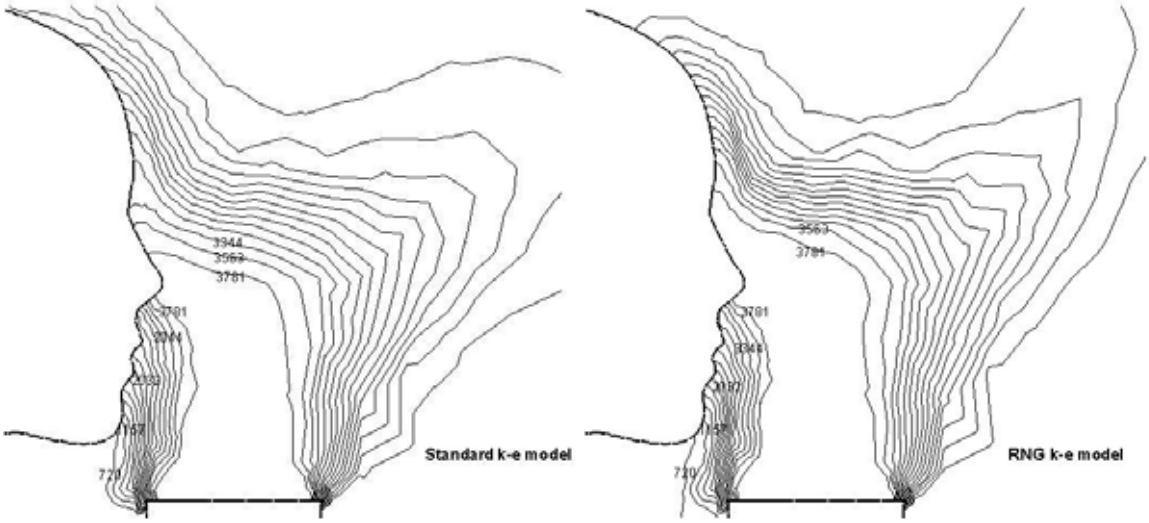

Figure 5 Tracer gas concentration contour (ppm) at the nose region (at the middle surface x=1.3 m)

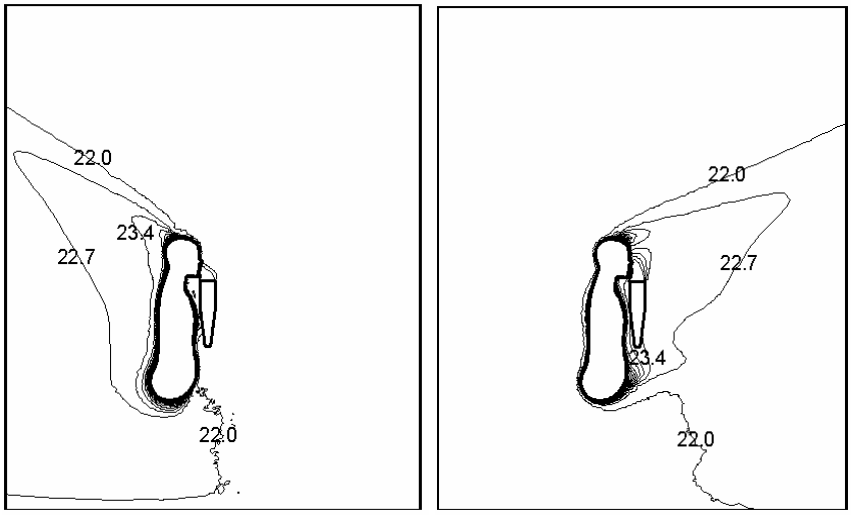

(a) From front *(b) From back*

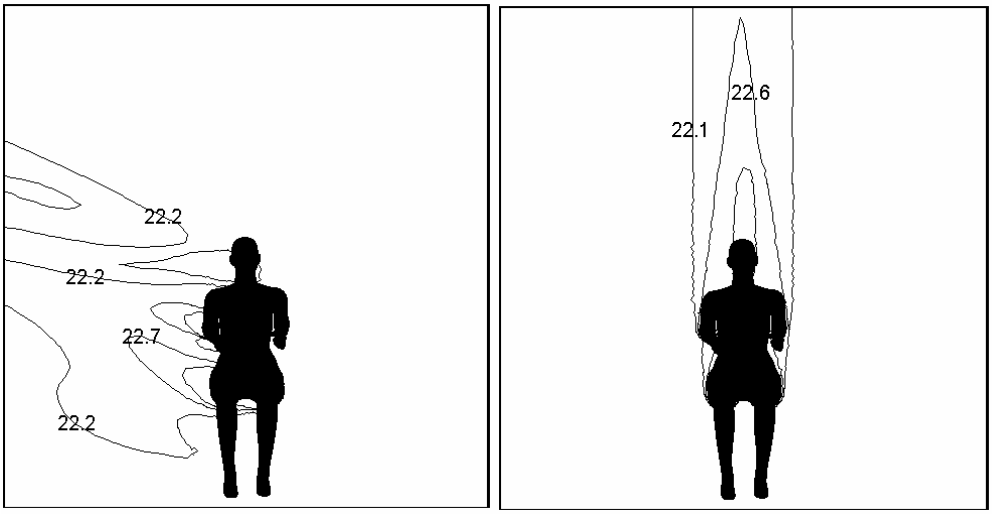

(c) From left *(d) From floor*

Figure 6 Temperature contours (℃) at different uniform airflow field

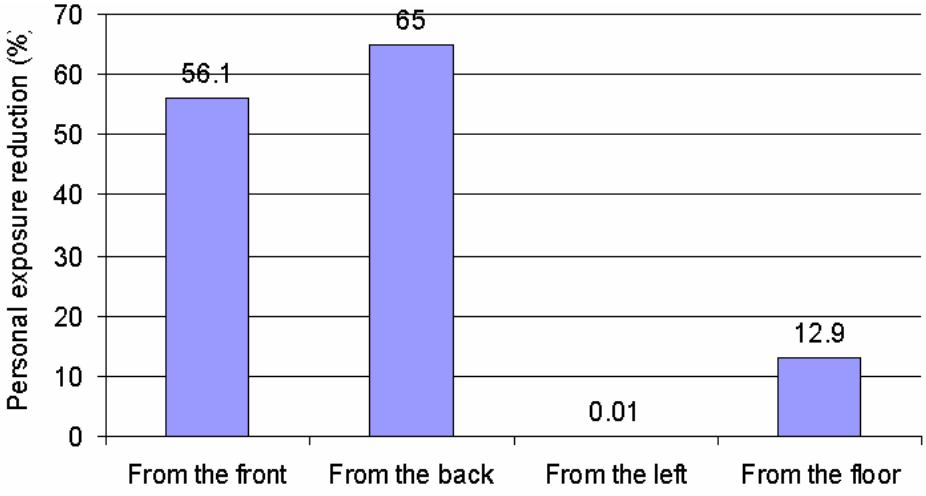

Figure 7 Comparison of PER under different uniform airflow

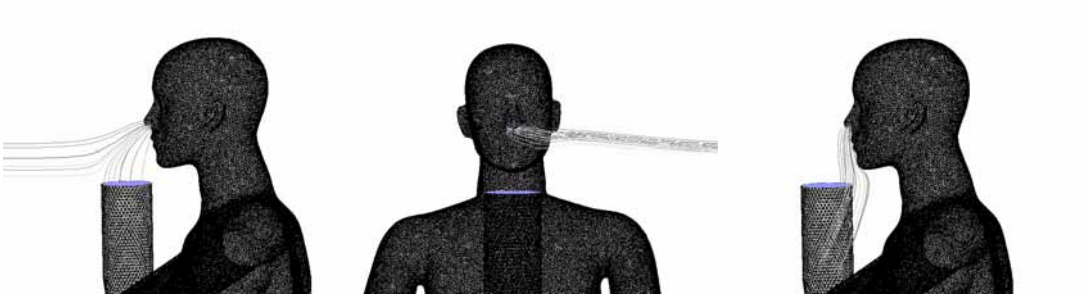

Figure 8 Path line of the inhaled air when the human body placed in a uniform airflow at the speed of 0.2m/s (the left one for airflow from the front; the middle one for airflow from the left; the right one for airflow from the back)

Table 1 Details of numerical methods and boundary conditions

Turbulence Model	Standard k-ε model
Numerical Schemes	Upwind second order difference; PISO algorithm; Steady state with full buoyancy effect; enhanced wall function.
Room Air Inflow	$V = 0.12m/s;\ T = 22\ ℃; C = 500ppm; I = 10\%;\ D = 0.335m$
Room Air Outflow	Pressure outlet
Room Wall	Adiabatic wall
Human Body	$T = 31\ ℃;$
Nose	$L = 0.14l/s; I = 10\%;\ D = 0.01m$
ATD Boundary	Adiabatic wall
ATD Outlet	$L = 0.8l/s;\ T = 20\ ℃; C = 4000ppm; I = 10\%;\ D = 0.08m$

Table 2 The different cases simulated

Name	Turbulence model	Room air supply method and velocity	Turbulence of room supply air
Case 1	Standard k-ε model	From supply opening V=0.12m/s	I=10%, D=0.335m
Case 2	RNG k- ε model	From supply opening V=0.12m/s	I=10%, D=0.335m
Case 3	Standard k- ε model	Left/right wall as room air inlet/outlet V=0.2m/s	I=10%, l=0.004m
Case 4	Standard k- ε model	Front/back wall as room air inlet/outlet V=0.2m/s	I=10%, l=0.004m
Case 5	Standard k- ε model	Back/front wall as room air inlet/outlet V=0.2m/s	I=10%, l=0.004m
Case 6	Standard k- ε model	Floor/ceiling as room air inlet/outlet V=0.2m/s	I=10%, l=0.004m